Evaluating Impacts of Recent Arctic Sea Ice Loss on the Northern Hemisphere Winter Climate Change

Fumiaki Ogawa, Noel Keenlyside, Yongqi Gao, Torben Koenigk, Shuting Yang, Lingling Suo, Tao Wang, Guillaume Gastineau, Tetsu Nakamura, Ho Nam Cheung, et al.

RESEARCH LETTER

Key Points:
- This study shows results from the first coordinated experiments on the sea ice impact for the observed climate change
- Climate change is coupled with sea ice loss only over the Arctic lower troposphere
- Models show that sea ice decline was not the cause of the recent colder winters over Siberia

Evaluating Impacts of Recent Arctic Sea Ice Loss on the Northern Hemisphere Winter Climate Change

Fumiaki Ogawa[1,2] (ID), Noel Keenlyside[1,2,3] (ID), Yongqi Gao[2,3] (ID), Torben Koenigk[4], Shuting Yang[5] (ID), Lingling Suo[2,3] (ID), Tao Wang[6] (ID), Guillaume Gastineau[7] (ID), Tetsu Nakamura[8] (ID), Ho Nam Cheung[1,2], Nour-Eddine Omrani[1,2], Jinro Ukita[9], and Vladimir Semenov[10,11]

[1]Geophysical Institute, University of Bergen, Bergen, Norway, [2]Bjerknes Centre for Climate Research, Bergen, Norway, [3]Nansen Environmental and Remote Sensing Center, Bergen, Norway, [4]Swedish Meteorological and Hydrological Institute, Norrköping, Sweden, [5]Danish Meteorological Institute, Copenhagen, Denmark, [6]Nansen-Zhu International Research Centre, Institute of Atmospheric Physics, Chinese Academy of Sciences, Beijing, China, [7]Sorbonne Universités/UPMC/CNRS/IRD, Paris, France, [8]Faculty of Earth Environmental Science, Hokkaido University, Sapporo, Japan, [9]Institute of Science and Technology, Niigata University, Niigata, Japan, [10]A.M. Obukhov Institute of Atmospheric Physics, Russian Academy of Sciences, Moscow, Russia, [11]Institute of Geography, Russian Academy of Sciences, Moscow, Russia

Abstract Wide disagreement among individual modeling studies has contributed to a debate on the role of recent sea ice loss in the Arctic amplification of global warming and the Siberian wintertime cooling trend. We perform coordinated experiments with six atmospheric general circulation models forced by the observed and climatological daily sea ice concentration and sea surface temperature. The results indicate that the impact of the recent sea ice decline is rather limited to the high-latitude lower troposphere in winter, and the sea ice changes do not significantly lead to colder winters over Siberia. The observed wintertime Siberian temperature and corresponding circulation trends are reproduced in a small number of ensemble members but not by the multimodel ensemble mean, suggesting that atmospheric internal dynamics could have played a major role in the observed trends.

Plain Language Summary Understanding the mechanism governing the ongoing global warming is a major challenge facing our society and its sustainable growth. Together with the CO_2-forced warming, the concurrent polar sea ice loss might also have contributed to the observed Arctic warming amplification and also to the cooling trends over Eurasia through a dynamical teleconnection. However, previous individual modeling studies suggest widely different findings on the role of sea ice loss in Northern Hemisphere climate change. To help resolve this controversy, we used satellite-derived sea ice and sea-surface temperature to run coordinated hindcast experiments with five different atmospheric general circulation models. The multimodel ensemble-mean results presented in the paper reduce biases of each model and eliminate atmospheric internal unforced variability, and thus provide the best estimate to date of the signal of the polar sea ice loss. The results suggest that the impact of sea ice seems critical for the Arctic surface temperature changes, but the temperature trends elsewhere seem rather due to either sea-surface temperature changes or atmospheric internal variability. They give clear guidance on how to provide society with more accurate climate change attributions. Our work is of interest to stakeholders of countries in the Northern Hemisphere middle and high latitudes.

1. Introduction

Arctic sea ice has significantly decreased under recent global warming and reached new record minimum extent during many months of 2016 (www.arctic-roos.org). Concomitantly, Arctic surface temperature rose about twice faster than at lower latitudes (Serreze & Barry, 2011). Meanwhile, the Siberian region cooled rather than warmed (Cohen et al., 2014). The mechanism for this "Warm Arctic and Cold Eurasia" teleconnection pattern (Mori et al., 2014) in winter is still under debate—previous studies have argued a possible impact of sea ice reduction in the Barents-Kara region through enhancement of Siberian High (Honda et al., 2009; Kim et al., 2014; Kug et al., 2015; Mori et al., 2014; Wang et al., 2017); impact of sea surface temperature (SST) changes in the Gulf Stream (Sato et al., 2014), the tropical Pacific (He et al., 2013), and the North Atlantic (Peings & Magnusdottir, 2014); or atmospheric internal variability (McCusker et al., 2016; Sorokina et al., 2016). It is difficult to evaluate relative importance and contributions from those various factors

because of the differences in experimental designs, models, and boundary forcing. In addition, the atmospheric circulation response to the Arctic sea ice changes could vary regionally and seasonally (Screen, 2017; Sun et al., 2015) and could be nonlinear (Overland et al., 2016; Semenov & Latif, 2015). This calls for multimodel coordinated experiments to better address the impacts of sea ice on the recent northern hemisphere climate change and to assess the relative contributions of Arctic sea ice, remote SST, and internal atmospheric dynamics. Here we present the first such experiments and synthesize the arguments from previous studies.

2. Coordinated Experiments

We conduct hindcast simulations of the recent 33 years (1982–2014) using atmospheric general circulation models forced by prescribed SST and sea ice from the National Oceanic and Atmospheric Administration (NOAA) Optimum Interpolation 1/4 Degree Daily Sea Surface Temperature Analysis version2, AVHRR-only product (Reynolds et al., 2007) (provided from http://www.ncdc.noaa.gov/sst/index.php). Two experiments are performed to distinguish the sea ice and SST impacts: Daily varying sea ice, exhibiting rapid reduction in the recent decades (Figure S1 in the supporting information), is prescribed in both experiments; daily varying SST is prescribed in the first experiment (SST-SIC-EXP), while daily climatological SST computed from the NOAA data is prescribed in the second (SIC-EXP). The climatology is computed following a previous study (Screen et al., 2013): In any grid box north of 40°N, if the daily mean SIC deviated from daily climatology by >10%, the grid box is set to observed SIC and SST; in all the grid boxes south of 40°N and at grid boxes north of 40°N where the daily mean sea ice concentration is within 10% of the climatological daily mean, observed SIC and climatological SST are used.

The two coordinated experiments are performed with five different models using different resolutions and parameterizations to account for model systematic errors: Community Atmosphere Model (CAM4; Neale et al., 2013) (0.9 × 1.25° with 26 vertical levels up to 3 hPa), WACCM (Marsh et al., 2013) (0.9 × 1.25° with 66 vertical levels up to 0.000006 hPa), IFS (Balsamo et al., 2009) (T255 with 91 vertical levels up to 0.01 hPa), IAP4 (Dong et al., 2012) (1.4 × 1.4° with 26 vertical models up to 10hPa), and LMDZOR (Hourdin et al., 2013) (2.5 × 1.25° with 39 vertical levels up to 0.04 hPa). Four of the above models were used to study Arctic climate change and variability in previous studies (e.g., Lang et al., 2017; Sun et al., 2015); these individual studies had different experimental designs and scientific foci. The experiments were repeated using different initial conditions to make 20 ensembles for each of the five different models (CAM4, WACCM, IFS, LMDZOR, and IAP4) in order to better consider internal atmospheric dynamics. The discontinuity in the NOAA daily data, caused by a change in the sea ice data source on 1 January 2005 (Reynolds et al., 2007), was corrected by specifying the same data-void regions through 2005 and onward. Also, two other obvious errors were corrected by linear interpolation of the daily anomalies (29 November 1987 to 18 January 1988 [SIC] and 27 April 2009 to 19 May2009). The last correction was not applied for the IFS model, but it did not affect the results notably. Furthermore, in order to evaluate the robustness of our results, an additional sensitivity experiment is performed with a sixth atmospheric model (AFES [Ohfuchi et al., 2004]; 1.5° × 1.5° with 56 levels up to 0.09 hPa) prescribing monthly mean SST and SIC from a different data set (Hurrel et al., 2008), simulating 30 ensemble members for both experiments. All experiments are conducted with transient forcing following the CMIP5 protocol (historical forcing from1982 to 2005 and the RCP8.5 scenario onward). These experiments were performed under the NordForsk funded GREENICE project (https://greenice.b.uib.no/), and the data including the corrected boundary condition are freely available (Ogawa et al., 2018; see reference).

3. Simulated Decadal Climate Changes

To investigate how much of the changes in Arctic near-surface (2 m) air temperature can be attributed to the prescribed boundary conditions, we compare the multimodel ensemble mean linear trend of the 2 m temperature to the ERA-interim reanalysis (Dee et al., 2011). In winter (December-January-February), the significant polar warming is rather localized (Figure 1a) and robust warming among different reanalysis data is found mainly at two centers in the northeast of Canada and the Barents-Kara sea regions; note that the warming signal in the East Siberian-Chukchi Sea region (130°E–160°E, 70°–80°N) is not robust among different reanalysis data, according to an intercomparison study (Lindsay et al., 2014). Both SST-SIC-EXP and SIC-EXP (Figures 1b and 1c) well simulate the two robust warming centers. Therefore, the observed significant near-surface warmings seems associated with the Arctic sea ice change. While the tropical Pacific has been linked to the warming over the northeast of Canada and Greenland (Ding et al., 2014), the simulated
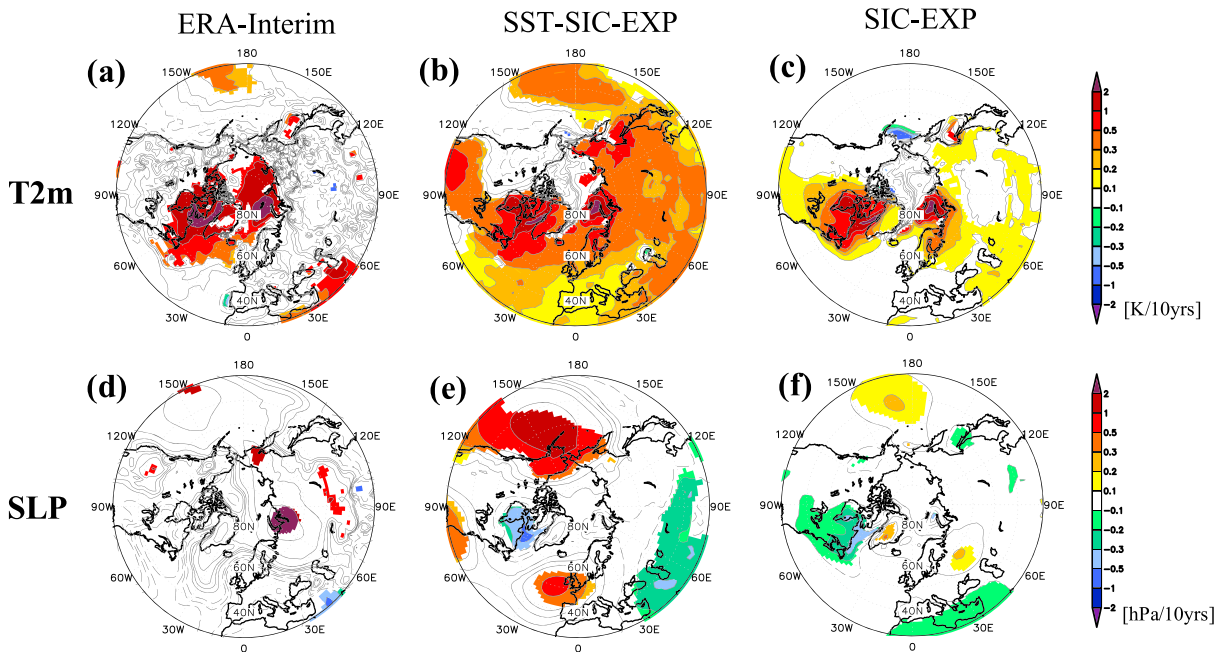
ERA-Interim   SST-SIC-EXP   SIC-EXP

Figure 1. (a–c) Mean observed 2 m temperature trends in DJF from 1982 to 2014. (a) For ERA-Interim and (b and c) for the simulated multimodel ensemble mean trends in SST-SIC-EXP and SIC-EXP, respectively. (d–f) As in (a)–(c), but for the SLP. The shading is applied for the statistical significance by a Student's *t* test with 95% confidence level.

significant warming signal in SIC-EXP (Figure 1c) suggests that the polar sea ice can largely explain such localized warming without the tropical SST changes. The mechanism for this regional warming will be further addressed in a future study. The time evolution of the simulated multimodel ensemble mean winter-mean polar surface temperature agrees well with the reanalysis for both of the SST-SIC-EXP and SIC-EXP (Figure S2). The individual model ensemble means also capture the long-term warming and much of the year-to-year variations in polar surface temperature, but they exhibit large mean differences to the reanalysis (Figure S2).

However, the simulated response to the SST and/or sea ice does not match the observed wintertime near-surface temperature trend over Siberia (Figures 1a–1c). Neither SST-SIC-EXP nor SIC-EXP shows a significant cooling trend in the 2 m temperature over Siberia; rather, SST-SIC-EXP shows a strong warming during 1982–2014 (~0.5 °C/decade). The observed Siberian cooling trend in the reanalysis is associated with the strengthening of the high-pressure system in northern Eurasia (McCusker et al., 2016; Sorokina et al., 2016) (Figures 1a and 1d). Neither of our experiments simulates the high-pressure trend around the observed location in the multimodel mean (Figures 1e and 1f), consistent with the absence of the significant cooling trends over Siberia (Figures 1b and 1c). It is still noteworthy that significant warming is absent over the Siberian region (centered at 95°E, 55°N) in SIC-EXP. This might be because the impact of increasing radiative forcing is suppressed by the climatological fixed SST; or it might indicate an impact of sea ice to reduce the warming over the Siberian region by forcing a corresponding high-pressure trend (Figure 1f). However, as we discuss later, it is unlikely that the sea ice reduction is the dominant cause of the observed Siberian cooling.

The multimodel ensemble mean reduces the amplitude of unforced signals compared to forced ones. Assuming our models correctly simulate the response to prescribed boundary and radiative forcing, the lack of a simulated Siberian wintertime cooling suggests that the observed changes are likely associated with internal atmospheric dynamics. In supporting this, the wintertime Siberian cooling is hardly statistically significant in the reanalysis because of large atmospheric interannual variability. Furthermore, the observed Siberian cooling is also associated with decadal changes of atmospheric internal variability patterns such as the Arctic Oscillation (AO) (Nakamura et al., 2015).

Our experiments suggest that the observed changes were rather unusual, as the Siberian cooling and associated surface high pressure trends with the observed amplitudes are rarely reproduced in individual members (Figures 2a and 2b). For 2 m temperature (and SLP), only 7 (and 2) of the total 260 members of
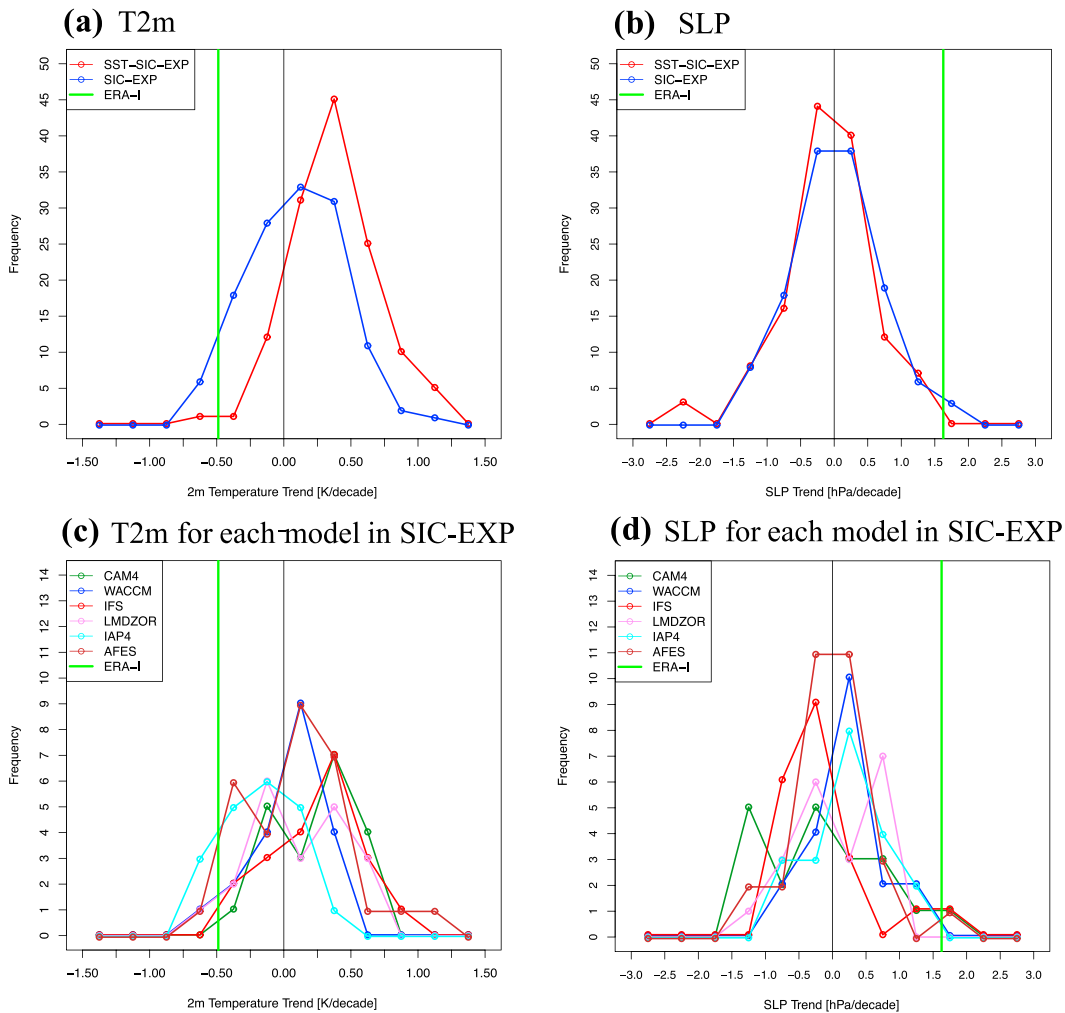
Figure 2. (a) Histogram of the linear trend of DJF-mean 2 m temperature averaged over the Siberian region (55°E–125°E 45°N–65°N). The unit of horizontal axis is [K/decade], and the vertical axis is the frequency. The red/blue diagram corresponds to the results of experiment with observed/climatological sea surface temperature, respectively. The green vertical line indicates the corresponding value in ERA-Interim. (b) As (a), but for sea level pressure averaged over the North Siberia region (40°E–100°E 50°N–80°N). (c and d) The lines are as in (a) and (b), but for the ensemble means of the individual models only for the SIC-EXP.

SST-SIC-EXP and SIC-EXP did reproduce the trends with observed amplitude, respectively. This is consistent with a previous numerical study which did not reproduce the cooling (McCusker et al., 2016). Nevertheless, 2 m temperature trends of the 5 individual members simulating the strongest Siberian cooling in SST-SIC-EXP and SIC-EXP (Figures 3b and 3c) show a dipole-like pattern of warmer Arctic and colder Siberia similar to the ERA-Interim (Figure 3a), and the accompanied intensification of the simulated SLP over northern Eurasia (Figures 3e and 3f) is also consistent with the reanalysis (Figure 3d). Thus, the intensification of the high-pressure system seems a driver for the Siberian cooling (Honda et al., 2009; McCusker et al., 2016) in these ensemble members, and the models appear able to simulate this type of observed variability.

No particular model appears to be preferred with respect to the members simulating strong Siberian wintertime cooling with an intensified high-pressure system (Figures 2c and 2d and Table S1a in the supporting information). It is indeed notable that the IAP4 model in SIC-EXP has a higher probability to simulate the Siberian cooling than other models (Figure 2c), with a statistically significant difference in its probability distribution (Table S1b). However, the corresponding distribution of SLP trend simulated in IAP4 is similar to other models (Figure 2d), and not significantly different (Table S1c).

The observed cooling trend over the Siberian region is associated with a wave train-like remote impact from the Barents-Kara sea region to the Siberian region (Honda et al., 2009). Previous studies suggest that this Rossby wave train is forced by heating over Barents-Kara Sea. The teleconnection through the wave train
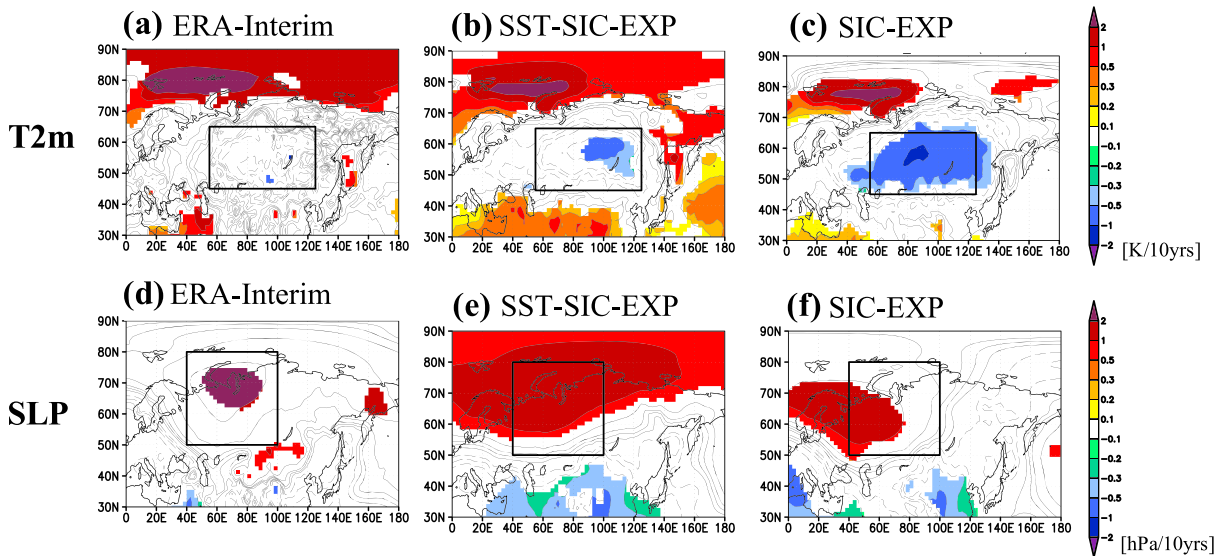
Figure 3. Linear trend of (a) 2 m temperature and (d) sea level pressure from 1982 to 2014 averaged in winter months (December-January-February) [/decade]. The black boxes indicate the region averaged to plot Figure 2. (b) Composited mean 2 m temperature trend of five individual ensembles simulating the coldest trends averaged in the box indicated by (a) for SST-SIC-EXP. (e) Composited mean sea level pressure trend of the same five individual ensembles as (b). (c and f) As (c) and (e) but for the SIC-EXP. The shading is applied for the statistical significance by a Student's *t* test with 95% confidence level.

can be addressed through the wave-activity flux (Takaya & Nakamura, 2001). We applied the diagnostic to the linear trend of 250 hPa geopotential height fields. Our results do not support the arguments by previous studies: A wave train pointing from the Barents-Kara sea region to the Siberian region (Figure S3a) is not reproduced in either of SST-SIC-EXP or SIC-EXP ensemble means (Figures S3b and S3c). However, an Arctic emanating wave train emanating is found in the individual members reproducing both cooling and warming over Siberia (Figures S3d–S3g). This means that the decadal temperature change over the Siberia could be influenced from the polar latitudes, regardless of the sign of the geopotential height anomalies and of the sea ice conditions. Thus, our results indicate that the sea ice reduction did not likely drive the recent observed Arctic emanating wave train that was linked to Siberian wintertime cooling.

Greater agreement with observations may be expected when observed changes in both SST and SIC are considered. However, our experiments suggest that SST changes reduced the chance for observed Siberian wintertime cooling. SIC-EXP shows higher probability to reproduce the cooling with the observed strength than SST-SIC-EXP (Figure 2a). The number of members simulating the negative trend over the Siberian region of interest is 14 (and 52) for SST-SIC-EXP (and SIC-EXP) out of the 130 members, respectively. The reduction in the number of members simulating the Siberian cooling trend in SST-SIC-EXP compared to SIC-EXP is robust to different area averages for the Siberian region and also among the different models used in this study (not shown). Indeed, the probability to reproduce the strengthening of the high-pressure system in northern Eurasia is higher in SIC-EXP (Figure 2b). Consistently, the multi-model ensemble mean of the wintertime sea level pressure trend over the northern hemisphere from SIC-EXP resembles the reanalysis better compared to SST-SIC-EXP, especially in the regions north of Siberia (Figures 1e and 1f). Unlike the reanalysis, SST-SIC-EXP shows a negative trend in sea level pressure northeastern America (60°W, 65°N) (Figure 1e), which is associated with a wave train-like pattern from lower latitudes in the Pacific (Figure S3b). Lower (or less high) geopotential height anomalies (or changes) in the polar region correspond to the positive AO as discussed through "polar cap height" in the previous studies (e.g., Kim et al., 2014; Wang et al., 2017). Therefore, the SST changes appear to reduce the probability to simulate the observed AO-like trend (Nakamura et al., 2015). Our results are robust to changes in the SST and SIC data used, as shown by simulations with another model driven by monthly mean data from another source (Reynolds et al., 2007) (Figure S4).

On the other hand, our results indicate that the regional wintertime warming trends over Greenland and northeastern Canada may have also been contributed by the tropical SST changes (Ding et al., 2014), though it does not dominate the warming forcing. Wintertime geopotential height trends near the tropopause and
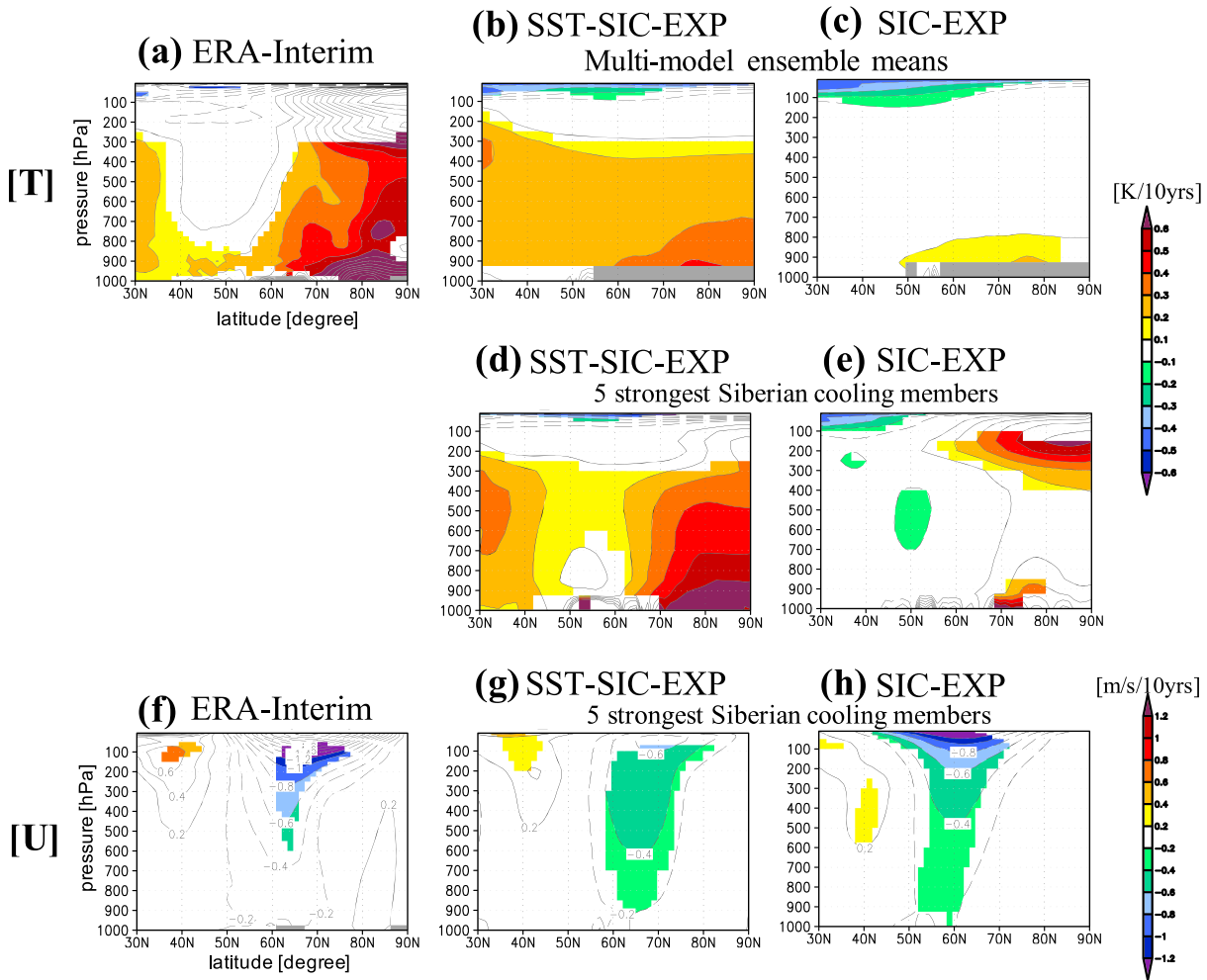
Figure 4. (a–c) DJF mean linear trend of zonal mean temperature from 1982 to 2014 for (a) ERA-Interim and the simulated multimodel ensemble mean trends in (b) SST-SIC-EXP and (c) SIC-EXP, respectively. (d and e) As in (b) and (c), but for the composite of the five members same as Figures 3b and 3c for SST-SIC-EXP and SIC-EXP, respectively. (f and g) As in (a), (d), and (e), but for the zonal mean zonal wind. The shading is applied for the statistical significance by a Student's *t* test with 95% confidence level.

corresponding wave-activity flux in the reanalysis (Figure S3a) and the multimodel mean of SST-SIC-EXP (Figure S3b) show evidence of the wavy pattern, which is associated with a southerly flow to the Greenland and northeastern Canada. However, SIC-EXP without tropical SST changes also shows geopotential-height pattern associated with a similar southerly flow to the regions (Figure S3c). In fact, the surface warming in the regions can be explained mostly without the tropical SST changes (Figures 1b and 1c).

Despite the difficulty in reproducing the Eurasian (central Asia) temperature/surface pressure trends, our experiments suggest that the polar sea ice reduction can partly cause the observed Arctic amplification (Gao et al., 2015; Graversen et al., 2008). In winter (December-January-February), the polar warming in the reanalysis is maximum near the surface and in the middle to upper troposphere with reduced warming in between (Figure 4a). This may suggest that the warming in the upper troposphere is not coupled with polar sea ice reduction, whose impact appears limited to the lower-most troposphere. Indeed, the near-surface warming signal is reproduced both in SST-SIC-EXP and SIC-EXP, while its upward extension is found only in the SST-SIC-EXP (Figures 4b and 4c). The lack of the upper-level warming in SIC-EXP (Figure 4c) suggests that the impact of sea ice is mainly confined to the surface and near the surface, consistent with previous numerical studies (Perlwitz et al., 2015; Screen et al., 2012). SST changes in the lower latitudes associated with the increasing greenhouse gases enhance the Arctic amplification of the upper tropospheric warming in addition to the impact of sea ice reduction, which is consistent with the previous coupled GCM runs forced by increasing CO_2 and the sea ice nudged to the climatology (McCusker et al., 2017). Although the simulated zonal-

mean surface warming is weaker than in the reanalysis, the horizontal surface warming structure itself is reasonably reproduced in the Arctic (Figures 1b and 1c). While the Arctic warming trend in the reanalysis in winter is associated with the increasing atmospheric thickness in the polar latitudes and the weakening of the midlatitude westerly (i.e., negative phase of the AO) (Kim et al., 2014; Nakamura et al., 2015), such westerly changes are not simulated in the SST-SIC-EXP or SIC-EXP ensemble mean (Figure S5).

However, the individual members that reproduce wintertime cooling in the Siberian continental regions similar to observed show a clearer "Arctic amplification" of the temperature warming and the negative AO-like zonal wind changes similar to observed (Figure 4). Furthermore, the teleconnection between the Barents-Kara Sea and Siberian regions through wave activity propagation is reasonably reproduced (Figures S3d and S3e). While the observed negative AO-like pattern, Arctic amplification, and Siberian cooling are dynamically related, they appear not to be caused by the observed SST and SIC changes as they are not reproduced by the ensemble mean.

4. Summary

In this study, we have shown through coordinated multimodel experiments that sea ice loss is unlikely to have led to colder winters over Siberia, while the global SST changes may have reduced the chance for such cold winters. Consistent with previous studies, the cooling of recent winters over Siberia is associated with the strengthening of the high-pressure system over northern Eurasia. Although a dynamical linkage between the sea ice loss and the Siberian cooling through the intensification of the Eurasian stationary high-pressure system (Honda et al., 2009) is found in a few ensemble members, the intensification of the high-pressure system is not likely a robust response to the sea ice loss. Thus, the Siberian cooling in the reanalysis seems dominated by the large interannual variability of atmospheric circulation. This inability to reproduce the Siberian temperature changes by prescribing Arctic Sea ice change is consistent with previous studies (Lang et al., 2017; Liu et al., 2012; McCusker et al., 2016). We also confirm that the Arctic amplification is strongly coupled with sea ice loss over the Arctic lower troposphere in winter, while the warming aloft is mostly associated with remote SST changes.

We find no evidence that the inability to reproduce the observed Siberian cooling and upper tropospheric polar changes is related to poor simulation of Arctic amplification. From our coordinated experiments, the warming tendency over the Arctic in each model shows good agreement to the reanalysis (Figure S2), while the simulated temperature response over Siberia differs from one model to another (Figure 2c) and only the IAP4 model simulates a cooling as the ensemble mean. The linear trends of the turbulent-heat fluxes (Figures S6 and S7) are rather similar among the models over the Arctic regions, and there is no striking difference in the case of IAP4 model. Further analysis of Arctic amplification is beyond the scope of this study.

Our overall results agree to another recent study (McCusker et al., 2016), which used a large number of simulations of just one model (CanESM2) with an additional coupling of the atmosphere and ocean. We further extend and strengthen the conclusions of the previous study by accounting for systematic error which is typically reduced in a multimodel mean. This is illustrated by evolution of the polar near-surface temperature (Figure S2) that are best captured by the multimodel ensemble mean. Ideally, such coordinated experiments need as many models as possible. We hope this study with six models may motivate further coordinated experiments using more models.

On the other hand, our results about the Arctic-Siberian teleconnection seem to contradict some previous studies using single AGCMs, which are not used in this study (e.g., CAM5 simulations (Kim et al., 2014) and ECHAM5 simulations (Wang et al., 2017)). The discrepancy could arise from the various factors as discussed below. In addition, it may be due to the fact that the Siberian temperature trend can be different from the interannual relationship of the Siberian temperature and the Barents-Kara sea ice anomalies (McCusker et al., 2016). This suggests that the interannual variability of the simulated Siberian temperature in the coordinated experiments and its relation to the prescribed Arctic sea ice should be addressed in a future study.

Our results have several implications left for future study. First, sea ice has a strong control on local climate, and therefore it deserves to be better observed and represented in models. The sea ice dataset used here was corrected for issues as discussed in the experimental design; this highlights a need for better quality controls in the present sea ice datasets. Second, the SST-driven teleconnections also need further investigation, as

they appear to reduce the chance of simulating the observed AO-like trend. Third, the simulated trends in this study could partly depend on the stratospheric representation of the climate models (Nakamura et al., 2015). Fourth, our experimental design did not resolve active ocean-atmosphere-sea ice coupling (Deser et al., 2015) or changes in sea ice thickness (Lang et al., 2017; McCusker et al., 2016), and these issues deserve further consideration in a coordinated manner. Lastly, climate models suggest a link between uncertainties in future change in pan-Arctic sea ice decline and Eurasian climate (Cheung et al., 2018); this implies potential differences between present and future changes. There are still conflicting results between this article and previous studies, which highlights a need for engaging community-wide, larger-scale numerical experiments incorporating the aforementioned issues.

References

Balsamo, G. P., Beljaars, A., Scipal, K., Viterbo, P., van den Hurk, B., Hirschi, M., & Betts, A. K. (2009). A revised hydrology for the ECMWF model: Verification from field site to terrestrial water storage and impact in the integrated forecast system. *Journal of Hydrometeorology*, *10*(3), 623–643. https://doi.org/10.1175/2008JHM1068.1

Cheung, H. H. N., Keenlyside, N. S., Omrani, N.-E., & Zhou, W. (2018). Remarkable link between projected uncertainties of Arctic sea-ice decline and winter Eurasian climate. *Advances in Atmospheric Sciences*, *35*(1). accepted. https://doi.org/10.1007/s00376-017-7156-5

Cohen, J., Screen, J. A., Furtado, J. C., Barlow, M., Whittleston, D., Coumou, D., et al. (2014). Recent Arctic amplification and extreme mid-latitude weather. *Nature Geoscience*, *7*(9), 627–637. https://doi.org/10.1038/ngeo2234

Dee, D. P., Uppala, S. M., Simmons, A. J., Berrisford, P., Poli, P., Kobayashi, S., et al. (2011). The ERA-Interim reanalysis: Configuration and performance of the data assimilation system. *Quarterly Journal of the Royal Meteorological Society*, *137*(656), 553–597. https://doi.org/10.1002/qj.828

Deser, C., Tomas, R. A., & Sun, L. (2015). The role of ocean-atmosphere coupling in the zonal-mean atmospheric response to Arctic Sea ice loss. *Journal of Climate*, *28*(6), 2168–2186. https://doi.org/10.1175/JCLI-D-14-00325.1

Ding, Q., Wallace, J. M., Battisti, D. S., Steig, E. J., Gallant, A. J. E., Kim, H.-J., & Geng, L. (2014). Tropical forcing of the recent rapid Arctic warming in northeastern Canada and Greenland. *Nature*, *509*(7499), 209–212. https://doi.org/10.1038/nature13260

Dong, X., Xue, F., Zhang, H., & Zeng, Q.-C. (2012). Evaluation of surface air temperature change over China and the globe during the twentieth century in IAP AGCM4.0. *Atmospheric and Oceanic Science Letters*, *5*(5), 435–438. https://doi.org/10.1080/16742834.2012.11447031

Gao, Y., Sun, J., Li, F., He, S., Sandven, S., Yan, Q., et al. (2015). Arctic sea ice and Eurasian climate: A review. *Advances in Atmospheric Sciences*, *32*(1), 92–114. https://doi.org/10.1007/s00376-014-0009-6

Graversen, R. G., Mauritsen, T., Tjernström, M., Källén, E., & Svensson, G. (2008). Vertical structure of recent Arctic warming. *Nature*, *451*(7174), 53–56. https://doi.org/10.1038/nature06502

He, S., Wang, H., & Liu, J. (2013). Changes in the relationship between ENSO and Asia-Pacific midlatitude winter atmospheric circulation. *Journal of Climate*, *26*(10), 3377–3393. https://doi.org/10.1175/JCLI-D-12-00355.1

Honda, M., Inoue, J., & Yamane, S. (2009). Influence of low Arctic sea-ice minima on anomalously cold Eurasian winters. *Research Letters*, *36*, L08707. https://doi.org/10.1029/2008GL037079

Hourdin, F., Foujols, M.-A., Codron, F., Guemas, V., Dufresne, J.-L., Bony, S., et al. (2013). Impact of the LMDZ atmospheric grid configuration on the climate and sensitivity of the IPSL-CM5A coupled model. *Geophysical Climate Dynamics*, *40*(9-10), 2167–2192. https://doi.org/10.1007/s00382-012-1411-3

Hurrel, J., Hack, J. J., Shea, D., Caron, J. M., & Rosinski, J. (2008). A new sea surface temperature and sea ice boundary dataset for the Community Atmosphere Model. *Journal of Climate*, *21*(19), 5145–5153. https://doi.org/10.1175/2008JCLI2292.1

Kim, B.-M., Son, S.-W., Min, S.-K., Jeong, J.-H., Kim, S.-J., Zhang, X., et al. (2014). Weakening of the stratospheric polar vortex by Arctic sea-ice loss. *Nature Communications*, *5*, 4646. https://doi.org/10.1038/ncomms5646

Kug, J.-S., Jeong, J.-H., Jang, Y.-S., Kim, B.-M., Folland, C. K., Min, S.-K., & Son, S.-W. (2015). Two distinct influences of Arctic warming on cold winters over North America and East Asia. *Nature Geoscience*, *8*(10), 759–762. https://doi.org/10.1038/ngeo2517

Lang, A., Yang, S., & Kaas, E. (2017). Sea ice thickness and recent Arctic warming. *Geophysical Research Letters*, *44*, 409–418. https://doi.org/10.1002/2016GL071274

Lindsay, R., Wensnahan, M., Schweiger, A., & Zhang, J. (2014). Evaluation of seven different atmospheric reanalysis products in the Arctic. *Journal of Climate*, *27*(7), 2588–2606. https://doi.org/10.1175/JCLI-D-13-00014.1

Liu, J., Curry, J. A., Wang, H., Song, M., & Horton, R. M. (2012). Impact of declining Arctic sea ice on winter snowfall. *PNAS*, *109*(11), 4074–4079. https://doi.org/10.1073/pnas.1114910109

Marsh, D. R., Mills, M. J., Kinnison, D. E., Lamarque, J.-F., Calvo, N., & Polvani, L. M. (2013). Climate change from 1850 to 2005 simulated in CESM1 (WACCM). *Journal of Climate*, *26*(19), 7372–7391. https://doi.org/10.1175/JCLI-D-12-00558.1

McCusker, K. E., Fyfe, J. C., & Sigmond, M. (2016). Twenty-five winters of unexpected Eurasian cooling unlikely due to Arctic sea-ice loss. *Nature Geoscience*, *9*, 838–842. https://doi.org/10.1038/ngeo2820

McCusker, K. E., Kushner, P. J., Fyfe, J. C., Sigmond, M., Kharin, V. V., & Bitz, C. M. (2017). Remarkable separability of circulation response to Arctic sea ice loss and greenhouse gas forcing. *Geophysical Research Letters*, *44*, 7955–7964. https://doi.org/10.1002/2017GL074327

Mori, M., Watanabe, M., Shiogama, H., Inoue, J., & Kimoto, M. (2014). Robust Arctic sea-ice influence on the frequent Eurasian cold winters in past decades. *Nature Geoscience*, *7*(12), 869–873. https://doi.org/10.1038/ngeo2277

Nakamura, T., Yamazaki, K., Iwamoto, K., Honda, M., Miyoshi, Y., Ogawa, Y., & Ukita, J. (2015). A negative phase shift of the winter AO/NAO due to the recent Arctic Sea-ice reduction in late autumn. *Journal of Geophysical Research Atmosphere*, *120*, 3209–3227. https://doi.org/10.1002/2014JD022848

Neale, R. B., Richter, J., Park, S., Lauritzen, P. H., Vavrus, S. J., Rasch, P. J., & Zhang, M. (2013). The mean climate of the Community Atmosphere Model (CAM4) in forced SST and fully coupled experiments. *Journal of Climate*, *26*(14), 5150–5168. https://doi.org/10.1175/JCLI-D-12-00236.1

Ogawa, F., Koenigk, T., Yang, S., Gastineau, G., Wang, T., Nakamura, T., & Suo, L. (2018). The outputs from GREENICE coordinated AGCM hindcast experiments driven by NOAA OI SST and sea ice data, Norstore research data archive. https://doi.org/10.11582/2018.00007

Ohfuchi, W., Nakamura, H., Yoshioka, M. K., Enomoto, T., Takaya, K., Peng, X., et al. (2004). 10-km mesh meso-scale resolving simulations of the global atmosphere on the Earth simulator—Preliminary outcomes of AFES (AGCM for the Earth simulator). *Journal of the Earth Simulator*, *1*, 8–34.

Overland, J. E., Dethloff, K., Francis, J. A., Hall, R. J., Hanna, E., Kin, S.-J., et al. (2016). Nonlinear response of midlatitude weather to the changing Arctic. *Nature Climate Change*, *6*(11), 992–999. https://doi.org/10.1038/nclimate3121

Peings, Y., & Magnusdottir, G. (2014). Forcing of the wintertime atmospheric circulation by the multidecadal fluctuations of the North Atlantic ocean. *Environmental Research Letters*, *9*(3), 034018. https://doi.org/10.1088/1748-9326/9/3/034018

Perlwitz, J., Hoerling, M., & Randall, D. (2015). Arctic tropospheric warming: Causes and linkages to lower latitudes. *Journal of Climate*, *28*(6), 2154–2167. https://doi.org/10.1175/JCLI-D-14-00095.1

Reynolds, R. W., Smith, T. M., Liu, C., Chelton, D. B., Casey, K. S., & Schlax, M. G. (2007). Daily high-resolution-blended analyses for sea surface temperature. *Journal of Climate*, *20*(22), 5473–5496. https://doi.org/10.1175/2007JCLI1824.1

Sato, K., Inoue, J., & Watanabe, M. (2014). Influence of the Gulf stream on the Barents Sea ice retreat and Eurasian coldness during early winter. *Environmental Research Letters*, *9*(8), 084009. https://doi.org/10.1088/1748-9326/9/8/084009

Screen, J. A. (2017). Simulated atmospheric response to regional and pan-Arctic Sea-ice loss. *Journal of Climate*, *30*(11), 3945–3962. https://doi.org/10.1175/JCLI-D-16-0197.1

Screen, J. A., Deser, C., & Simmonds, I. (2012). Local and remote controls on observed Arctic warming. *Geophysical Research Letters*, *39*, L10709. https://doi.org/10.1029/2012GL051598

Screen, J. A., Simmonds, I., Deser, C., & Tomas, R. (2013). The atmospheric response to three decades of observed Arctic sea ice loss. *Journal of Climate*, *26*(4), 1230–1248. https://doi.org/10.1175/JCLI-D-12-00063.1

Semenov, V. A., & Latif, M. (2015). Nonlinear winter atmospheric circulation response to Arctic sea ice concentration anomalies for different periods during 1966–2012. *Environmental Research Letters*, *10*(5), 054020. https://doi.org/10.1088/1748-9326/10/5/054020

Serreze, M. C., & Barry, R. G. (2011). Processes and impacts of Arctic amplification: A research synthesis. *Global and Planetary Change*, *77*(1-2), 85–96. https://doi.org/10.1016/j.gloplacha.2011.03.004

Sorokina, S. A., Li, C., Wettstein, J. J., & Kvamstø, N. G. (2016). Observed atmospheric coupling between Barents Sea ice and the warm-Arctic cold-Siberian anomaly pattern. *Journal of Climate*, *29*(2), 495–511. https://doi.org/10.1175/JCLI-D-15-0046.1

Sun, L., Deser, C., & Tomas, R. A. (2015). Mechanisms of stratospheric and tropospheric circulation response to projected Arctic Sea ice loss. *Journal of Climate*, *28*(19), 7824–7845. https://doi.org/10.1175/JCLI-D-15-0169.1

Takaya, K., & Nakamura, H. (2001). A formulation of a phase-independent wave-activity flux for stationary and migratory Quasigeostrophic eddies on a zonally varying basic flow. *Journal of the Atmospheric Sciences*, *58*, 608–627. https://doi.org/10.1175/1520-0469(2001)058%3C0608:AFOAPI%3E2.0.CO;2

Wang, S.-Y. S., Lin, Y.-H., Lee, M.-Y., Yoon, J.-H., Meyer, J. D. D., & Rasch, P. J. (2017). Accelerated increase in the Arctic tropospheric warming events surpassing stratospheric warming events during winter. *Geophysical Research Letters*, *44*, 3806–3815. https://doi.org/10.1002/2017GL073012